Low-frequency in the Default Mode Brain Network from Spiking Neuron Model

Teruya Yamanishi, Jian-Qin Liu, *Member, IEEE,* Haruhiko Nishimura, *Member, IEEE,* and Sou Nobukawa

***Abstract*—The approaches for regarding the functional characteristics of the brain as the dynamical behavior of a multi-scale neural system using neural network models are continued to attempt since fluctuations on blood–oxygen–level–dependent (BOLD) signals of the brain at a rate lower than 0.1 Hz have been observed by functional magnetic resonance imaging (fMRI) machines under the dozing situation. We construct a complex brain network model by functionally connecting neural clusters composed of spiking neurons with a complex network. By transducing to BOLD signals from firing patterns obtained by our new model, the network dynamics of the neural system and its behavior are quantitatively discussed.**

***Keywords*—Default-mode brain network, BOLD signals, Slow synchronizations, Neural network, Time delay.**

I. Introduction

TRADITIONALLY, the brain in the same way as the body has been thought to be in the state of resting for subjects in a doze, namely for the state of no task. At the same time, it has been implied that the brain consumes energy at 10 times the rate of the resting body per gram of tissue [1]. This value corresponds approximately to 20% of the total energy in the body when a person is at rest, though the human brain is only 2% of the weight of the body [2], [3]. As the average power consumption of typical adult is about 100 Watts, that of the brain becomes 20 W. The energy consumption of the brain is too large in proportion of active regions for neurons considered so far for the doze. So, this is referred to as "dark energy" in the words of astrophysics, and is the one of puzzles on the Brain Science, which can not be solved so far [4].

Recently, the functional magnetic resonance imaging (fMRI) machines allow observations of the brain for the long-time range at a much higher resolution than ever before, and the measurements of the blood–oxygen–level–dependent (BOLD) signal in the brain for the dozing situation propose a solution to the dark energy problem of the brain. The observations have revealed a broad active region with changing of the activity at the very slow frequency, which has been a spatiotemporally correlated synchronization at a rate lower than 0.1 Hz [5]–[7] and a functionally connected coactivation of multiple regions in cerebral cortex. At present, this state is so-called "default mode brain network" [8], where the default means that the brain under unfocused on the external environment, namely in the absence of an explicit task, is keeping on wide ranges of the activity. So why does the multiple regions active in spite of the rest state ? We infer that the center of the brain activity is a network consisting of several regions and, the network is considered to bring the neural activity variety together in a synchronized rhythm in order to correspond the events that may occur from now [6], [8]. Namely, the brain is working at a plurality of regions each while tuning in a resting state. Hence, the energy that is spent in the activities of the brain in that state reaches to about 20 times the energy expended on conscious task [4]. This large energy is seemed to be consistent with the dark energy of the brain. Here we show functional connecting core regions suggested as architectonics of the DMN in Table I, and imply the regions represented by Brodmann's areas at Fig.1.

At present, much knowledge and information on the DMN have been obtained from experiments using measuring instruments on the brain. For example, it can be predicted before the 30 minutes from the observation of the activities of the DMN, which the subject is whether or not to miss [9]. Also, the abnormal DMN has been reported to be associated with neurological disorders such as Alzheimer's disease or depressions. The area of the brain atrophy in patients with Alzheimer's disease almost overlaps with core regions of the DMN [10]–[12]. Thus, the DMN is inferred to carry an important role in order to oversee the activities of the brain, and investigations on brain activity at the DMN rest can be expected to provide new clues for understanding brain function and neurological disease. As mentioned above, experimental results or phenomena on the DMN have been reported, but a theoretical explanation of the generation mechanism of the DMN has not yet been established.

In this work, we suggest a complex brain network model based on the Izhikevich spiking neuron model for nerve cells of the cerebral cortex, and calculated raster plots for each core region of the DMN. From our calculations, the firing patterns of the spiking neuron model are mapped to the neuron assemblies corresponding to different regions of the brain, from which we estimate the proprieties of the network model. It is considered that this approach contributes to a better understanding of the overall activities of the relevant cortex regions rather than focusing on the activities of each neuron at the microscopic level. Furthermore, as slow fluctuations in

T. Yamanishi and H. Nishimura were supported by Grant-in-Aids for challenging Exploratory Research (23650357) and for Scientific Research (B-24300206 and C-22500638) from the Japan Society for the Promotion of Science, respectively. Also, J.-Q. Liu was supported by the funds from the National Institute of Information and Communications Technology.

T. Yamanishi is with the Department of Management Information Science, Fukui University of Technology, Fukui, 910–8505 JAPAN e-mail: yamanisi@fukui-ut.ac.jp .

J.-Q. Liu is with the National Institute of Information and Communications Technology, Kobe, 651–2492 JAPAN e-mail: liu@nict.go.jp .

H. Nishimura and S. Nobukawa are with the Graduate School of Applied Informatics, University of Hyogo, Kobe, 650–0047 JAPAN e-mails: haru@ai.u-hyogo.ac.jp, and ab10y406@ai.u-hyogo.ac.jp, respectively.

DOI: 10.5176/2251-3043_3.1.224

TABLE I
CORE REGIONS OF THE DEFAULT MODE BRAIN NETWORK. THE CORRESPONDING BRAIN AREAS GENERALLY IMPLY BRODMANN'S AREAS FROM REFS.[5], [8].

Regions	Abbreviation	Corresponding brain areas
Lateral temporal cortex	LTC	21
Medial prefrontal cortex	MPFC	24, 32ac, 10m/10r/10p, 9
Inferior parietal lobule	IPL	39, 40
Posterior cingulate cortex/ restrosplenial cortex	PCC/Rsp	23/31, 26,29,30
Parahippocampal cortex	PHC	36
Hippocampal formation	HF	–

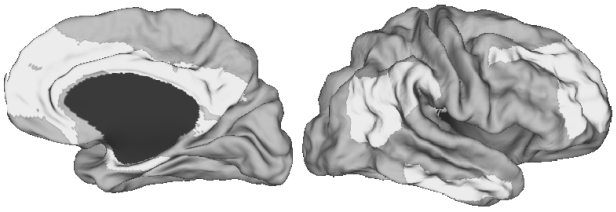

Fig. 1. The Brodmann's areas corresponding to the core regions in Table I are mapped by colored white.

BOLD signals are observed by fMRI under the DMN, firing patterns of active neurons obtained from our new model are transduced to the fluctuations in BOLD signals.

In the next section, we explain the spiking neuron model used here and the network structure in order to connect between neurons. The construction of a model on the default mode brain network and simulations are carried out in Section III. By using the values of parameters obtained here, we also estimate dependencies of strength of input stimulus on the model. Section IV describes on a hemodynamics model transforming the firing pattern of the neurons into fluctuations of BOLD signals, and Section V is devoted to summary and some discussions.

II. SPIKING NEURON MODEL AND NETWORK STRUCTURE

In 2003, Izhikevich has proposed a neuron model with firing patterns represented by simultaneous linear ordinary differential equations with four variables [13]. Their equations derive the membrane potential v [mV] of a neuron for the input current I flowing into the neuron, and are described as follows:

$$\frac{dv(t)}{dt} = 0.04\ v(t)^2 + 5\ v(t) + 140 - u(t) + I\ , \qquad (1)$$

where u is the recovery variable related to ion permeation of the membrane of neuron, which is given by

$$\frac{du(t)}{dt} = a\ (b\ v(t) - u(t))\ . \qquad (2)$$

The parameters a and b determine the time scale of u and the sensitivity of u to v, respectively. Moreover, if the value of v exceeds the pre-specified firing threshold (V_{th}), v is returned to the value of the resting membrane potential c, and an inactivity

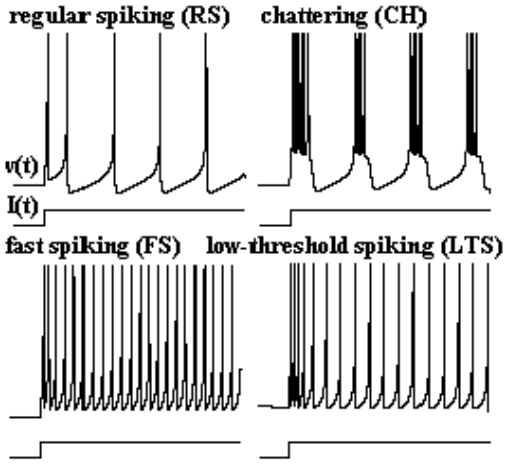

Fig. 2. Firing patterns of neurons in the Izhikevich model of Ref. [13].

period d is added to u. Fig.2 shows typical firing patterns of an excitatory neuron and an inhibitory neuron in this model.

For the constructing a model on the default mode brain network that is our purpose here, we need discuss on not only the neuron model but also the network structure because the brain is organized as neuron assemblies with hierarchies of complex network connectivity [14], [15]. At present, the network structure can be generally classified graphs as follows:

- Complete graph
  A network in which each node is linked to all other nodes.
- Random graph[16]
  A network in which two randomly selected nodes are linked with a certain binding rate.
- Watts − Strogatz (WS) model (small-world model)[17]
  A network in which the average distance (the average number of nodes) between nodes is small, and the clustering (proportion of nodes adjacent to a random node that are also adjacent to each other) is high.
- Scale free model[18]
  A network in which, in addition to small average distance and high clustering, the number of links from a node follows a power law.

Examples of these graphs with 20 nodes are shown in Fig.3.

Let us consider a network of neuron assemblies using Izhikevich's spiking neuron model. 800 excitatory neurons and 200 inhibitory neurons are placed randomly in a simple, and each neuron is also randomly coupled to all the others, namely the random graph as shown at the top right in Fig.3. Coupling strengths s_{ij} (i and j are the indices of the receiving and firing neurons, respectively) are assigned a uniformly random value, which is between 0 and 0.5 for firing by an excitatory neuron, and -1 and 0 for an inhibitory neuron. Then, (1)–(2) can be rewritten as [15]

$$\begin{aligned}\frac{dv_i(t)}{dt} &= 0.04\ v_i(t)^2 + 5\ v_i(t) + 140 - u_i(t) \\ &\quad + I_i + \sum_{j=\mathrm{Firing}} s_{ij}\ , \end{aligned} \qquad (3)$$

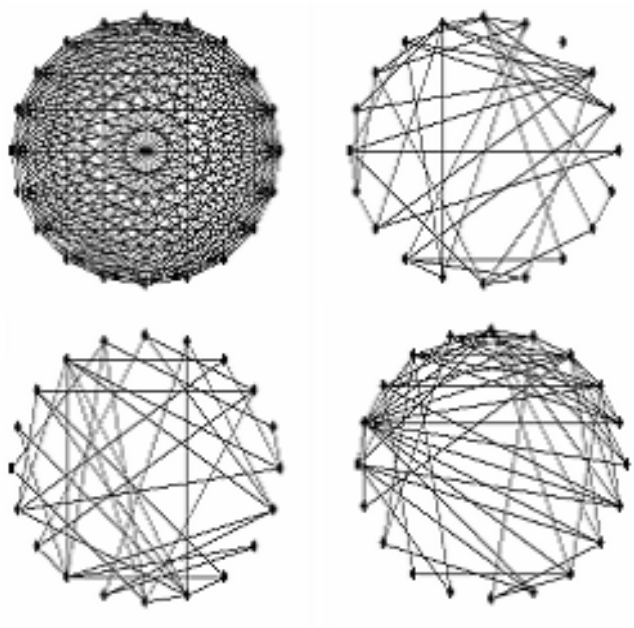

Fig. 3. Graphs of typical networks. In the top row are complete (left) and random (right) graphs; in the bottom row are Watts-Strogatz (left) and scale free (right) models.

$$\frac{du_i(t)}{dt} \quad = \quad a_i \ (b_i \ v_i(t) - u_i(t)) \ , \tag{4}$$

for the ith neuron, where $v_i \leftarrow c_i$, and $u_i \leftarrow u_i + d_i$ for $v_i > V_{i\ th}$ in the same as (2). The values of other parameters included in (3) and (4) are shown in Table II. The symbol $-$ in the table shows that a random value between the lower and upper limits is taken. For example, for the time scale a of an inhibitory neuron, a random value between 0.02 and 0.1 would be taken.

The result of the simulation experiment is shown in Fig.4 as firing patterns indicated by a black point, when a neuron is firing. Here the input current I_i flowing into the ith neuron in (3) is given as

$$I_i = k_i \cdot R(m = 0, \sigma^2 = 1) \ , \tag{5}$$

with a Gaussian random number $R(m, \sigma^2)$ at a mean m and a standard deviation σ. k_i represents a strength of the stimulus, and is taken as 5 and 2 for the excitatory and the inhibitory ith neuron, respectively, by considering the sensitivity of the stimulus for different neurons. One can see an alpha rhythm ($\sim$ 10 Hz) appears very early, and a gamma rhythm ($\sim$ 40 Hz) of even shorter cycle appears approximately 500 ms later. This agrees with the results of Izhikevich[13]. Taking into account the fact that synchronization can arise from the assembly of this spiking neuron model, we proceed to apply this model to study the dynamic behavior of the brain's default mode network, and attempt to understand the mechanism of how fast local dynamics in the alpha and/or gamma rhythms for the neurons emerge the slow 0.1 Hz fluctuations as typical signature of the resting brain.

III. Model and Simulation

Based on such functionally connected system of the brain in Fig.1, we assume that the cortex region is composed of the

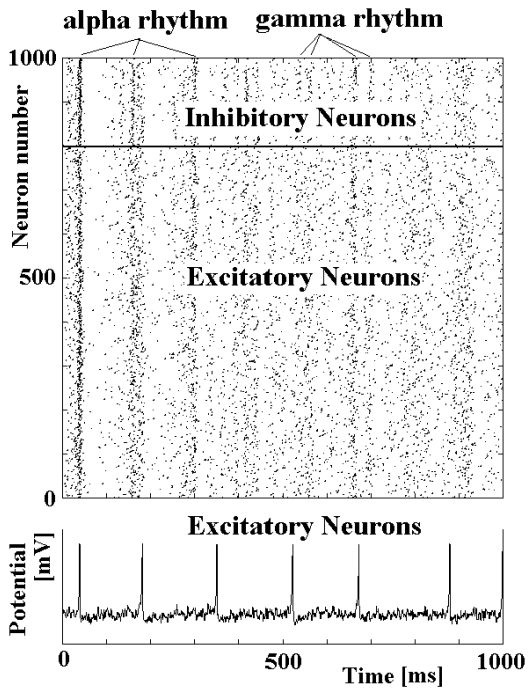

Fig. 4. Simulations of a randomly coupled network with 1000 Izhikevich spiking neurons. Top: spike raster plot with 800 excitatory neurons and 200 inhibitory ones. Bottom: typical spike train of an excitatory neuron.

TABLE II
Parameter values of the Izhikevich neuron model used in our simulations.

Parameters	Excitatory neuron	Inhibitory neuron
Time scale a	0.02	$0.02 - 0.10$
Sensitivity b	0.20	$0.20 - 0.25$
Resting membrane potential c	$-65 - -50$	-65
Inactivity period d	$2 - 8$	2

neuron assembly formed by placing 160 excitatory neurons and 40 inhibitory neurons in one dimension, and construct a new neural network with the spiking neuron model for the default mode brain network. The ratio of the excitatory neuron's number to the inhibitory one in the region is fixed to follow that of anatomical insight for the human brain. In addition, the neural network takes into account 2 different intrinsic properties as follows:

- Hierarchic neuroanatomical connectivity structure
  - Neuron assembly in each region
    The network is taken to be randomly coupled with the strengths as shown at the graph of the top right in Fig.3 because if neurons in the brain are connected by a complete network, the capacity of the brain would be so large that it could not placed in our head.
  - Collective regions in clusters
    The coupling strength between each region is given as the functional correlation one with the

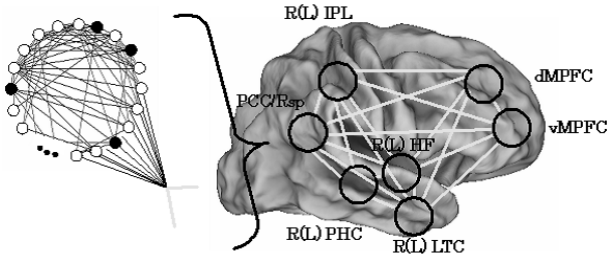

Fig. 5. A network model with the spiking neuron model on the default mode brain network is illustrated. Each region has 200 spiking neurons with intra-connections, and is functionally connected at correlation strengths from anatomical analyses with inter-connections indicated by colored white. The open and closed circles in left indicate the excitatory neuron and inhibitory neuron, respectively. The solid-line circles on the image of the brain represent core areas of the default mode brain network indicated in Table I.

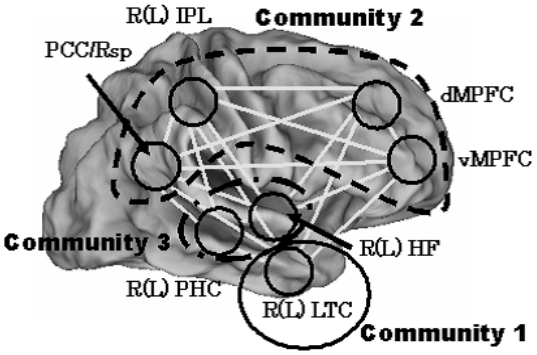

Fig. 6. The core regions suggested as default mode brain network are collected into three communities. The community 1, 2, and 3 are depicted with the solid line, the dashed line, and the dash-dotted line including each region, respectively.

default mode brain network, which is named an *inter*-connection here. On the other hand, we call an *intra*-connection the coupling strength between each neuron.

The conceptual diagram of new neural network with this hierarchic structure is shown in Fig.5.

- Time delay in the transmission of information [19], [20]
  The delay is simply considered as temporal transmission, and obtained by a common propagation velocity and 3D Euclidean distance between any 2 different regions. Then, we take the velocity as a parameter v, and estimate the distance from the typical locations of the regions in 3D space from the human data.

Taking into account these intrinsic properties, the membrane potential of the ith neuron in the M-region for the synaptic current I_{Mi} flowing into its neuron is extended to

$$\frac{dv_{Mi}(t)}{dt} = 0.04\ v_{Mi}(t)^2 + 5\ v_{Mi}(t) + 140 - u_{Mi}(t) + I_{Mi}\ , \quad (6)$$

with

$$I_{Mi} = I_i + \sum_{Mj=\text{Firing}} s_{MiMj} + \mu \sum_{N(N\neq M)} C_{MN}\ x_N(t-\tau_{MN})\ , \quad (7)$$

where s_{MiMj}, C_{MN}, and μ in (7) are taken as the strengths of intra-, inter-connections, and the parameter of the coupling strength for the inter-connection, respectively. I_i is an input current and is given by (5). The first two terms in (7) are Izhikevish terms with the pulse-coupled implementation, and last term is newly introduced by the inter-connection between regions. The value of C_{MN} is taken same value as Fig. 8 of Ref. [8], and is shown in Table III. In (7), the first sum is a sum of the coupling strength between the firing pre-synaptic neuron j and the post-synaptic neuron i in the region M at time t, and its strength generally depends to the strength of the synaptic current. Here the coupling strength of s_{MiMj} is simply taken as an independence of the synaptic current and a random number. x_N is the firing rate of the region N and is written by the amount of the firing neuron to the total neuron on N at time t. Also, τ_{MN} is the time delay from the region N to M [19]:

$$\tau_{MN} = \frac{L_{MN}}{v_0}\ , \quad (8)$$

where v_0 and L_{MN} are the velocity as parameter and typical distance between regions M and N, respectively.

For simulation experiments, we use the result of hubs and subsystem within the default mode brain network mapped and estimated from functional connectivity analysis as C_{MN} in (6). As a result, our each region now is regarded as in the functional connectivity region in the brain. The other parameters in (6)–(8) are taken as same values on simulations of 1000 neuron case shown in Table II.

Now, we examined raster plots in our default mode brain network. Then, the result is implied as one for clusters of communities collecting some regions. Because fMRI data on the default mode brain network is not observed at each core region, but at functional collective region constructed by core regions, it is important to carry out the simulation experiments on the power spectrum of the signals of the communities clustered core regions by the strength of the functional correlation. So we collect eleven regions into three communities by taking into account strengths of the correlation between regions given at Table III as follows:

- Community 1 : L LTC and R LTC regions
  The functional attribution of these regions is the memory and learning.
- Community 2 : dMPFC, vMPFC, L IPL, R IPL, and PCC/Rsp regions
  These regions carry the cognition, integration of sensory information, and so on.
- Community 3 : L PHC, R PHC, L HF, and R HF regions
  Here is the memory encoding and retrieval, and long-term memory.

We graphically represent three communities composed of some core regions with lines at Fig.6. For their communities we show results on raster plots in Fig.7 for the parameter of the coupling strength for the inter-connection $\mu = 49$ in (7) and the velocity $v_0 = 78$ mm/ms in (8).

Next, we find the behavior of this model at large stimulus, which corresponds the wakefulness from the doze. For a large

TABLE III
FUNCTIONAL CORRELATION STRENGTHS OF EACH REGION WITHIN THE DEFAULT MODE NETWORK [8], [**?**].

Nodes	L LTC	R LTC	dMPFC	vMPFC	L IPL	R IPL	PCC/Rsp	L PHC	R PHC	L HF	R HF
L LTC	1.00	0.41	0.16	0.12	0.14	0.12	0.12	0.11	0.06	0.18	0.14
R LTC		1.00	0.16	0.18	0.07	0.20	0.19	0.08	0.10	0.15	0.17
dMPFC			1.00	0.47	0.22	0.31	0.34	−0.06	−0.10	−0.01	−0.04
vMPFC				1.00	0.27	0.31	0.52	0.11	0.06	0.20	0.16
L IPL					1.00	0.47	0.49	0.25	0.10	0.11	0.06
R IPL						1.00	0.42	0.12	0.05	0.09	0.07
PCC/Rsp							1.00	0.23	0.16	0.26	0.21
L PHC								1.00	0.57	0.31	0.28
R PHC									1.00	0.28	0.28
L HF										1.00	0.61
R HF											1.00

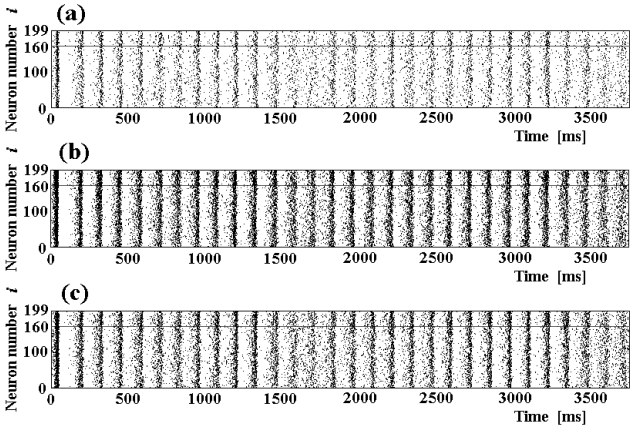

Fig. 7. Spike raster plot of each community under the doze state from 0 to 3750 ms with $\mu = 49$ and $v_0 = 78$ mm/ms. The dots means the neuron i with firing at t where the neuron i is in the core region M of any community. In the core region, the neuron numbers from 0 to 159 and from 160 to 199 represent excitatory and inhibitory neurons in each core region, respectively. A line in figure differentiates the areas of excitatory and inhibitory neurons. Figures (a), (b), and (c) correspond to the community 1 (L LTC and R LTC regions), 2 (dMPFC, vMPFC, L IPL, R IPL, and PCC/Rsp regions), and 3 (L PHC, R PHC, L HF, and R HF regions), respectively.

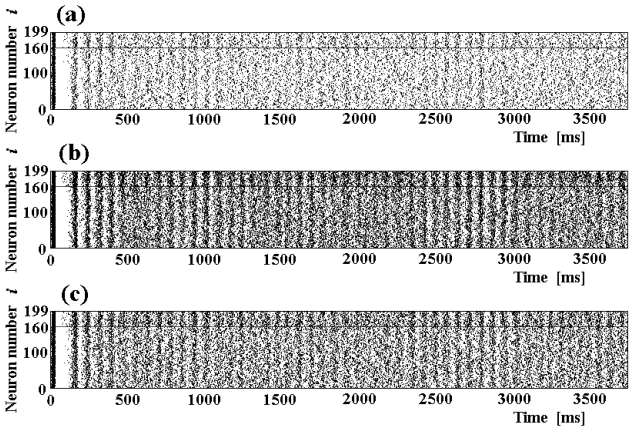

Fig. 8. Same as Fig.7 except for the strength of the stimulus giving to neurons. The strength of the stimulus is set 1.5 times larger than case of the doze state. It is found that neurons both spatially and temporally fire more than Fig.7 because of the large stimulus.

value of the input current I_i in (5), where the values of k_i are given as 7.5 and 3 for the ith excitatory and inhibitory neuron, respectively, raster plots for the communities are shown in Fig.8 by using the same parameter values as in Fig.4. The firing patterns of our model for the large I_{Mi} become to be synchronized both spatially and temporally for each community.

We also attempt to simulate on the model under a lack of properties on the brain. When the time delay in the transmission of information is simply considered as temporal transmission, it is brought by the finite propagation velocity between neurons. So, we vanish the time delay by taking the infinite of the velocity in (8). The result of raster plots is shown in Fig.9 at same values of the synaptic current I_{Mi} and parameters as case of Fig.7. The synchronization of the neuron firing spatially and temporally becomes stronger as in case of large stimulus.

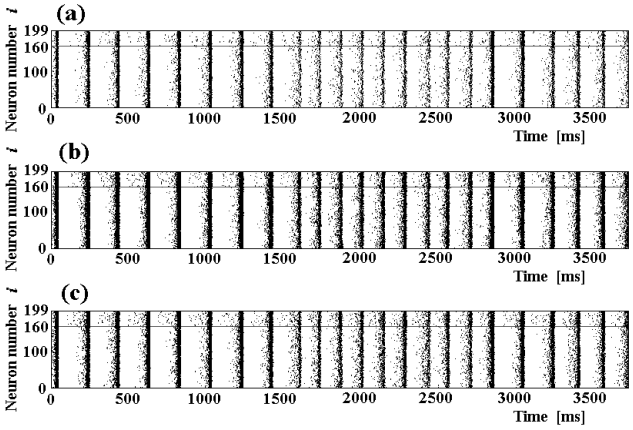

Fig. 9. Same as Fig.7 except for the time delay raised by transmitting of information between core regions. For the lack of the time delay, we can see that synchronizations of this case become stronger than ones of the doze state since the neuron is strongly mutually interfere with each other by transmitting instantaneously the stimulus from other firing neurons.

IV. Transformation of BOLD signals from firing patterns

In previous sections, we estimated the raster plots of the default mode brain network using Izhikevich's spiking neuron model. However, in order to accurately compare the fluctuation obtained our brain model with the result of fMRI measurements, the firing pattern of the neurons arising from our brain network model should be transformed into fluctuations of BOLD signals. So, let us consider to calculate BOLD signals using Balloon–Windkessel hemodynamics model which specifies the coupling of perfusion to the BOLD signals [23], [24].

In the measurement principle of fMRI, when the neural activity becomes more active, the consumption of oxygen in that area is increased. Then, the blood volume increases to expand the blood vessels in order to avoid oxygen deficiency due to consumption of oxygen, and the increase in blood flow in blood vessels is measured as an increase of the BOLD signal. For the neuron signal $N_i(t)$ in the region M at the time t, the neuron activity causes an increase in a vasodilatory signal $s_{Mi}(t)$ that is subject to an autoregulatory feedback. Inflow of blood $f_{Mi}(t)$ and outflow $f_{Mout}(t)$ correspond in proportion to this signal with concomitant changes in blood volume $V_{Mi}(t)$ and deoxyhemoglobin content $q_{Mi}(t)$. These variables are represented by differential equations and given by [24]

$$\begin{aligned} \frac{ds_{Mi}(t)}{dt} &= N_i(t) - \kappa\, s_{Mi}(t) - \gamma_{Mi}\,(f_{Mi}(t) - 1)\ , \\ \frac{df_{Mi}(t)}{dt} &= s_{Mi}(t)\ , \\ \lambda_{Mi}\frac{dV_{Mi}(t)}{dt} &= f_{Mi}(t) - f_{Mout}(t)\ , \\ \lambda_{Mi}\frac{dq_{Mi}(t)}{dt} &= \frac{f_{Mi}(t)\ E(f_{Mi},\rho_{Mi})}{\rho_{Mi}} - \frac{f_{Mout}(t)\ q_{Mi}(t)}{V_{Mi}(t)}\ . \end{aligned} \tag{9}$$

Here $E(f_{Mi},\rho_{Mi})$ in (9) is a function of flow for the oxygen extraction with the resting oxygen extraction fraction $\rho_{Mi} = 0.8$ at the active neuron i in the region M, and $f_{Mout}(t)$ is related to $V_{Mi}(t)$ with Grubb's exponent $\alpha = 0.2$, $f_{Mout}(t) = V_{Mi}^{1/\alpha}(t)$ [25]. Also, the biophysical parameters κ, γ_{Mi}, and λ_{Mi} in (9) are a rate of signal decay, a rate of flow-dependent elimination, and a hemodynamic transit time, respectively. We put $\kappa = 1.25$, $\gamma_{Mi} = 2.5$, and $\lambda_{Mi} = 1$ [24]. Taking the BOLD signal as a static nonlinear function of volume and deoxyhemoglobin that comprises a volume-weighted sum of extra- and intra-vascular signals, the BOLD signal $y_{Mi}(t)$ is given by

$$\begin{aligned} y_{Mi}(t) &= V_0 \left\{ \varepsilon_1 \Big(1 - q_{Mi}(t)\Big) + \varepsilon_2 \Big(1 - \frac{q_{Mi}(t)}{V_{Mi}(t)}\Big) \right. \\ &\quad \left. + \varepsilon_3 \Big(1 - V_{Mi}(t)\Big) \right\} + y_0\ , \end{aligned} \tag{10}$$

with

$$\varepsilon_1 = 7\rho_{Mi}\ , \qquad \varepsilon_2 = 2\ , \qquad \varepsilon_3 = 2\rho_{Mi} - 0.2\ , \tag{11}$$

where V_0 is resting blood volume fraction and is taken as 0.02 [24], and y_0 the initial condition.

By the way, as fMRI is the measurement of cerebral blood flow changes with time corresponding to the stimulation the extraction on active region of neurons is obtained by using the t-test method, difference method, or the correlation method. Considering the difference method for simplicity on the fluctuations of neuron firing patterns simulated from (6)–(8) shown in Figs.7–9 to the BOLD signal, we introduce an order parameter for the region M [19]:

$$K_M(t_f) = \frac{K'_M(t_f) - < K'_M(t_f) >}{< K'_M(t_f) >}\ , \tag{12}$$

where $<>$ denotes the average over time, and

$$K'_M(t_f) = < |\Sigma_{i\in M} F_i(t) - < \Sigma_{i\in M} F_i(t) > | > \ , \tag{13}$$

with $F_i(t)$ representing the neuron firing i in the region M at the time t. $K_M(t_f)$ is obtained in a sliding time window shifted by step time, where each time window starts at time t_i and ends at time t_f. For neuron i, $F_i(t)$ is considered as 1 for firing and 0 for no firing. Note that $<>$ in (13) is the average taken over each time window. As K_M describes the change in the ratio of the amount of firing neurons to the average at each time window, the magnitude of K_M is smaller when firing neurons begin to be fickle spatiotemporally. On the other hand, the more the firing neurons localize spatially, the greater the magnitude of K_M.

Calculating the order parameter K_M in (12) by using neuron firing patterns in Fig.7 simulated from (6)–(8) and substituting K_M obtained here for the neuron signal N_i in (9), we engender fluctuations of BOLD signals from our brain network model. For the community 1 we show the result of the BOLD signal on K_M in (12) at the parameter of the coupling strength for the inter-connection $\mu = 49$ in (7) and the velocity $v_0 = 78$ mm/ms in (8) in Fig.10. Here, it notes that the power spectrum on the BOLD signal is derived by the fluctuation of one over 15 seconds because our fluctuations of the BOLD signal obtained from three differential equations (9) are unstable for the initial time. From this figure, we can find that our model of the default mode brain network has the slow fluctuation at < 0.1 Hz and consists with the observed behavior of the BOLD signal on the default mode network of the brain with no task. This result is derived that synchronized firing patterns of each core region through the intra-connection between neurons become to be weak alpha rhythms but no gamma ones at the rest state as the doze condition, and cluster communities arise synchronous firings with the slow fluctuation of the rate lower than 0.1 Hz by time delay in propagating local synchronizations created at each core region through the inter-connection.

Similarly, Figs.11 and 12 are the results of the BOLD signal for the large stimulus and the lack of time delay by using neuron firing patterns in Figs.8 and 9, respectively. In case of the large stimulus in Fig.8, the power spectrums peak of K_M sharply arounds the frequencies of the alpha rhythms, and the fluctuations at less than 0.1 Hz are relatively small. Our brain network model reproduce a fact well, which neurons become to active and raise the alpha rhythms ($5 - 10$ Hz) under any stimulus. However, the power spectrums peak of the BOLD signal has no frequencies with the alpha rhythms, and becomes

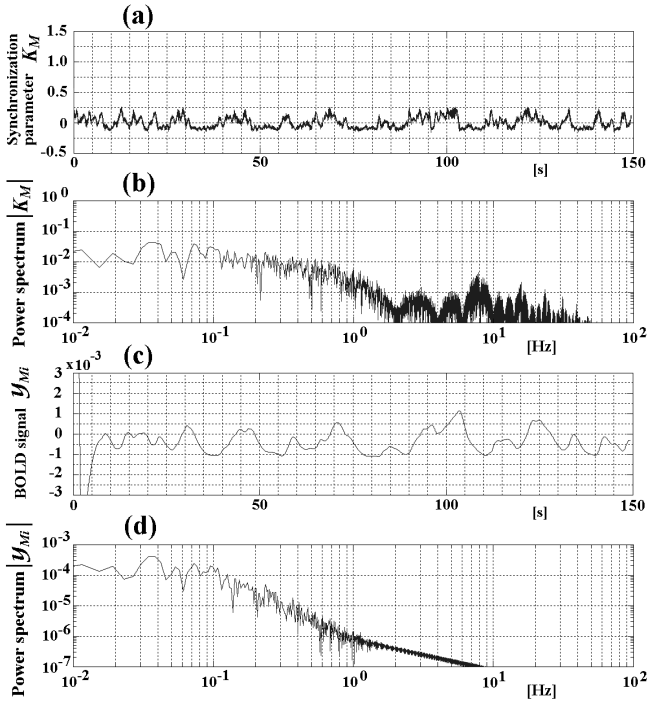

Fig. 10. (a) Behavior of the fluctuation parameter K_M in a term of the time t in (12) obtained from simulated neuron firing activities in Fig.7 for community 1 with $\mu = 49$ and $v_0 = 78$ mm/ms. (b) Power spectrum of K_M for community 1. The vertical and horizontal axes are both logarithmic scales. The power spectrum peaks for the fluctuations at low frequencies (< 0.1 Hz). (c) Result of the BOLD signal y_{Mi} in a term of the time t in (10) derived from the parameter K_M of community 1. (d) Power spectrum on y_{Mi} for community 1. The calculation result reveals the peak of the power spectrum at < 0.1 Hz on the fluctuation of the BOLD signal. Then, the power spectrum is estimated at $t \leq 15$ [s] because our BOLD signal obtained from three differential equations (9) are unstable for the initial time.

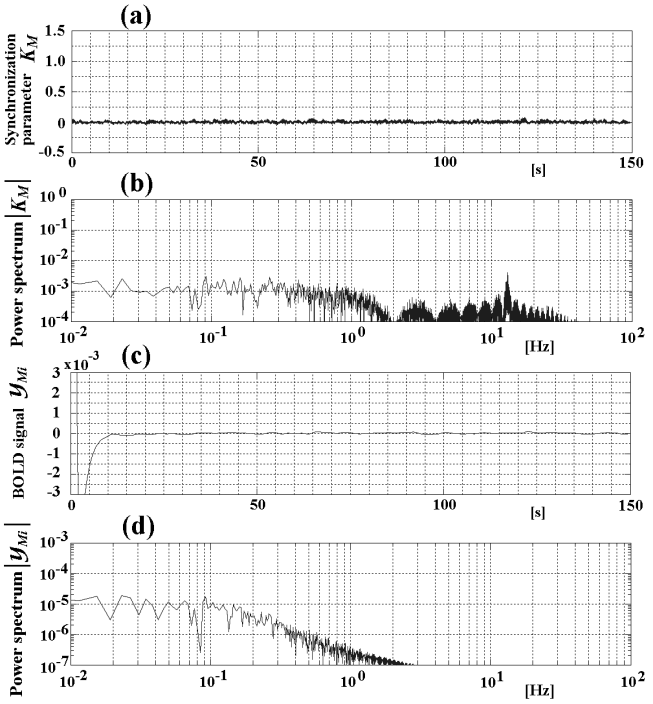

Fig. 11. (a) Behavior of the fluctuation parameter K_M in a term of the time t in (12) obtained from simulated neuron firing activities in Fig.8 for community 1 under the large stimulus with $\mu = 49$ and $v_0 = 78$ mm/ms. The value of the strength of the stimulus k_i included the input current I_i in (5) is put at 1.5 times more than that for case of Fig.10. The values of other parameters are same for case of Fig.10. (b) Power spectrum of K_M for community 1. The vertical and horizontal axes are both logarithmic scales. The power spectrum peak also arises for the alpha rhythm region. It shows that the strength of the power spectrum at < 0.1 Hz is almost same as an order of one at the alpha rhythm. (c) Result of the BOLD signal y_{Mi} in a term of the time t in (10) derived from the parameter K_M of community 1 under the large stimulus. (d) Power spectrum on y_{Mi} for community 1. The calculation result vanishes the peak of the power spectrum at the alpha rhythm on the fluctuation of K_M. As the temporal resolution of fMRI is the order of a few seconds, the BOLD signal cannot respond to the high frequencies.

at near 0.1 Hz. As well-known, the temporal resolution of fMRI is the order of a few seconds, and the BOLD signal cannot respond in real time to the firing of neurons. The vanish of the peak of the spectrum of the BOLD signal with the alpha rhythms proves that the transformation model from firing patters of neurons to the BOLD signal used here is legitimate.

Moreover, the results on the power spectrums peak of K_M and the BOLD signal on the lack of the time delay are shown in Fig.12, and also are similar as those on the large stimulus. For the result on K_M, the power spectrum declines steadily for frequencies less than 0.04 Hz; in contrast, the strength increases in Fig.10. This result suggests that the peak fluctuation at < 0.1 Hz is formed from the dilution of different rhythms of synchronization generated in each region by certain transmission delay for finite propagation velocity. Here the transmission is proportional to the product of the strength of the interconnection and the number of firing neurons inside each region. Therefore, the transmission with no delay enhances the synchronization of the intrinsic rhythm generated by each region, and the intrinsic synchronizations of each region strongly and directly affect the fluctuation in the firing pattern for communities.

V. Summary and Future Work

We simulated the power spectrum of communities clustered from raster plots of the default mode network with eleven core regions functionally connected using Izhikevich's spiking neuron model. In estimations with neurons having a random connection in each node as the network structure, the fluctuation of the BOLD signal has peaked in the region with < 0.1 Hz. The result agrees with fMRI data of the brain for experiments under the doze. However, the power spectrums of the order parameter K_M on firing patterns of neurons under the large stimulus or the lack of the time delay between core regions of the default mode brain network have disappeared the peaks of frequencies with < 0.1 Hz though those of the BOLD signal barely kept around 0.1 Hz. From these results, we found that the time delay on the transmission of information between core regions carried out a role on one of functions on the brain, namely default mode brain network state. Also, the analysis of the BOLD signal was only difficult to distinguish neuron activities of the doze state from ones with the large stimulus because of the temporal resolution of fMRI.

In this work, both the connections among neurons in each

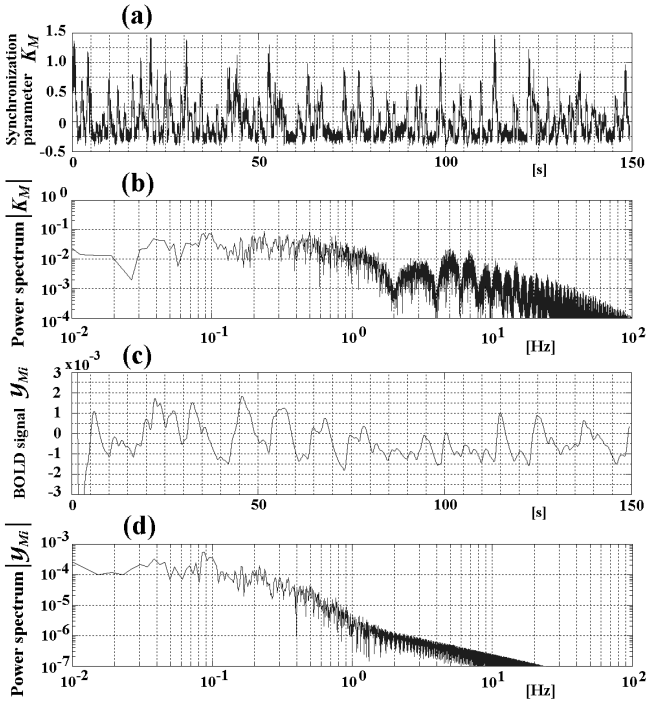

Fig. 12. (a) Behavior of the fluctuation parameter K_M in a term of the time t in (12) obtained from simulated neuron firing activities in Fig.9 for community 1 with the lack of the time delay at $\mu = 49$ and $v_0 = 78$ mm/ms. The values of other parameters are same for case of Fig.10. (b) Power spectrum of K_M for community 1. As in Fig.10, the vertical and horizontal axes are both logarithmic scales. In contrast of Fig.10, the value of the power spectrum does not become larger as the value of frequency becomes small. (c) Result of the BOLD signal y_{Mi} in a term of the time t in (10) derived from the parameter K_M of community 1 with the lack of the time delay. (d) Power spectrum on y_{Mi} for community 1. The calculation result reveals no increase in the peak of the power spectrum at < 0.1 Hz.

core region and those among core regions in the default mode network are simply considered as the random graph [16], but one generally infers a relation to the network of Watts-Strogatz [17] or the scale free [18] for the network of the brain [21], [22]. So it is important to explore the dependence of firing patterns and the power spectrum on a topology of the network structure in our model.

REFERENCES

[1] P. Wolfe, "Brain Matters: Translating Research into Classroom Practice," Assn for Supervision & Curriculum, 2001.

[2] L. Hart, "How the Brain Works," New York: Basic Books, 1975.

[3] G. Brown, "The Energy of Life," New York: Free Press, 1999.

[4] D.-Y. Zhang and M. E. Raichle, "Disease and the brain's dark energy," *Nature Reviews Neurology*, 6, 2010, pp. 15–28.

[5] M. D. Fox, A. Z. Snyder, J. L. Vincent, M. Corbetta, D. C. Van Essen, and M. E. Raichle, "The human brain is intrinsically organized into dynamic, anticorrelated functional networks," *PNAS*, 102, 2005, pp. 9673–9678.

[6] M. D. Fox and M. E. Raichle, "Spontaneous fluctuations in brain activity observed with functional magnetic resonance imaging," *Nature Reviews of Neuroscience*, 8, 2007, pp. 700–711.

[7] M. F. Mason, M. I. Norton, J. D. Van Horn, D. M. Wegner, S. T. Grafton, and C. N. Macrae, "Wondering Minds: The default Network and Stimulus-Independent Thought," *Science*, 315, 2007, pp. 393–395.

[8] R. L. Buckner, J. R. Andrews-Hanna, and D. L. Schacter, "The Brain's Default Network: Anatomy, Function, and Relevance to Disease," *Ann. N. Y. Acad. Sci.*, 1124, 2008, pp. 1–38.

[9] K. D. Singha and I.P. Fawcettb, "Transient and linearly graded deactivation of the human default-mode network by a visual detection task," *NeuroImage*, 41, 2008, pp. 100–112.

[10] M. D. Greicius, G. Srivastava, A. L. Reiss, and V. Menon, "Default-mode network activity distinguishes Alzheimer's disease from healthy aging: Evidence from functional MRI," *PNAS*, 101, 2004, pp. 4637–4642.

[11] V. D. Calhoun, T. Eichele, and G. Pearlson, "Functional Brain Networks in Schizophrenia: A Review," *Front. Hum. Neurosci.*, 3, 2009, pp. 17-1–17-12.

[12] M. Boly, T. Tshibanda, A. Vanhaudenhuyse, Q. Noirhomme, C. Schnakers, D. Ledoux, P. Boveroux, C. Garweg, B. Lambermont, C. Phillips, A. Luxen, G. Moonen, C. Bassetti, P. Maquet, and S. Laureys, "Functional connectivity in the default network during resting state is preserved in a vegetative but not in a brain dead patient," *Human Brain Mapping*, 30, 2009, pp. 2393–2400.

[13] E. M. Izhikevich, "Simple Model of Spiking Neurons," *IEEE Trans. Neural Networks*, 14, 2003, pp. 1569–1572.

[14] E. Bullmore and O. Sporns, "Complex brain networks: graph theoretical analysis of structural and functional systems," *Nature Reviews Neuroscience*, 10, 2009, pp. 186–198.

[15] T. Yamanishi and H. Nishimura, "Firing Correlation in Spiking Neurons with Watts-Strogatz Rewiring," *Natural Computing*, Springer, 2010, pp. 363–371.

[16] P. Erdös and A. Renyi, "On random graphs," *Publ. Math.* (Debrecen), 6, 1959, pp. 290–297.

[17] D. J. Watts and S. H. Strogatz, "Collective dynamics of 'Small-world' networks," *Nature*, 393, 1998, pp. 440–442.

[18] A. -L. Barabási and R. Albert, "Emergence of scaling in random networks," *Science*, 286, 1999, pp. 349–352.

[19] G. Deco, V. Jirsa, A. R. McIntosh, O. Sporns, and R. Kötter, "Key role of coupling, delay, and noise in resting brain fluctuations," *PNAS*, 106, 2009, pp. 10302–10307.

[20] A. Ghosh, Y. Rho, A. R. McIntosh, R. Kötter, and V. K. Jirsa, "Noise during Rest Enable the Exploration of the Brain's Dynamic Repertoire," *PLoS Comput. Biol.*, 4, 2008, e1000196.

[21] D. S. Bassett and E. Bullmore, "Small-World Brain Networks," *The Neuroscientist*, 12, 2006, pp. 512–523.

[22] L. Zemanová, C. Zhou, and J. Kurths, "Structural and functional clusters of complex brain networks," *Physica D*, 224, 2006, pp. 202–212.

[23] K. J. Friston, A. Mechelli, R. Turner, and C. J. Price, "Nonlinear Responses in fMRI: The Balloon model, Volterra kernels, and Other Hemodynamics," *NeuroImage*, 12, 2000, pp. 466–477.

[24] K. J. Friston, L. Harrison, and W. Penny, "Dynamic causal modelling," *NeuroImage*, 19, 2003, pp. 1273–1302.

[25] R. L. Grubb, M. E. Rachael, J. O. Euchring, and M. M. Ter-Pogossian, "The effects of changes in PCO2 on cerebral blood volume, blood flow and vascular mean transit time," *Stroke*, 5, 1974, pp. 630–639.

Teruya Yamanishi received the Master's degree in educations of science from Kobe University in 1991, and the Ph.D. degree in physics from Kobe University in 1994. He is a Professor at Fukui University of Technology where he studies mathematical information science for the brain, and develops optimization tools on behaviors of the autonomous robots.

Jian-Qin Liu received the Ph.D. degree in industrial automation (control science and engineering) from Central South University, Changsha, China, in 1997 and the Ph.D. degree in informatics from Kyoto University, Kyoto, Japan, in 2006. He is currently a Senior Researcher at Advanced ICT Research Institute, National Institute of Information and Communications Technology, Kobe, Japan. He is a Vice Co-chair of Nano-Scale, Molecular, and Quantum Networking Subcommittee of Emerging Technologies Committee, IEEE Communications Society, an Area Associate Editor of Special Issues on Emerging Technologies in Communications: Area 8 "Nanoscale and Molecular Networking," IEEE Journal on Selected Areas in Communications. He is a member of the IEEE P1906.1 standards working group.

Haruhiko Nishimura graduated from the Department of Physics, Shizuoka University in 1980 and completed the doctoral program at Kobe University, and received the Ph.D. degree in 1985. He is a Professor of the Graduate School of Applied Informatics, University of Hyogo and the Dean of the Graduate School of Applied Informatics and the Director of the information science research center for social applications, University of Hyogo. He is currently serving as a Committee Member of the "Task Force on Complex-valued Neural Networks," IEEE Computational Intelligence Society, and as a Member of the editorial board of the Journal of the Society of Kansei Engineering. He was awarded ISCIE paper prize in 2001 and JSKE paper prize in 2010.

Sou Nobukawa received the Bachelor's degree in science from University of Ryukyus and the Master's degree in science from University of Hyogo. He is currently working towards his Ph.D. degree under the supervision of Prof. Nishimura. His research interests include chaos, neural networks, and software engineering.